OXFORD

SOT | Society of Toxicology
www.toxsci.oxfordjournals.org

TOXICOLOGICAL SCIENCES, 151(1), 2016, 193–203

doi: 10.1093/toxsci/kfw035
Advance Access Publication Date: February 15, 2016
Research Article

Cardiac-Specific Deletion of the *Pdha1* Gene Sensitizes Heart to Toxicological Actions of Ischemic Stress

Wanqing Sun,[*,†] Nanhu Quan,[*,†] Lin Wang,[*,†] Hui Yang,[†] Dongyang Chu,[†] Quan Liu,[*] Xuezhong Zhao,[*] Jiyan Leng,[*,1] and Ji Li[†]

[*]The First Affiliated Hospital of Jilin University, Changchun 130000, China and [†]Department of Physiology and Biophysics, University of Mississippi Medical Center, Jackson, MS 39216

[1]To whom correspondence should be addressed at the First Affiliated Hospital of Jilin University, Changchun 130000, China. Fax: 86-431-8878-2217. Email: jiyanleng2013@163.com.

ABSTRACT

Pyruvate dehydrogenase (PDH) plays a key role in aerobic energy metabolism and occupies a central crossroad between glycolysis and the tricarboxylic acid cycle. We generated inducible cardiac-specific PDH E1α knockout ($CreER^{T2}$-$PDH^{flox/flox}$) mice that demonstrated a high mortality rate. It was hypothesized that PDH modulating cardiac glucose metabolism is crucial for heart functions under normal physiological and/or stress conditions. The myocardial infarction was conducted by a ligation of the left anterior descending coronary arteries. Cardiac PDH E1α deficiency caused large myocardial infarcts size and macrophage infiltration in the hearts ($P < .01$ vs wild-type [WT]). Wheat germ agglutinin and Masson trichrome staining revealed significantly increased hypertrophy and fibrosis in PDH E1α-deficient hearts ($P < .05$ vs WT). Measurements of heart substrate metabolism in an *ex vivo* working heart perfusion system demonstrated a significant impairment of glucose oxidation in PDH E1α-deficient hearts during ischemia/reperfusion ($P < .05$ vs WT). Dichloroacetate, a PDH activator, increased glucose oxidation in WT hearts during ischemia/reperfusion and reduced myocardial infarct size in WT, but not in PDH E1α-deficient hearts. Immunoblotting results demonstrated that cardiac PDH E1α deficiency leads to an impaired ischemic AMP-activated protein kinase activation through Sestrin2-liver kinase B1 interaction which is responsible for an increased susceptibility of PDH E1α-deficient heart to ischemic insults. Thus, cardiac PDH E1α deficiency impairs ischemic AMP-activated protein kinase signaling and sensitizes hearts to the toxicological actions of ischemic stress.

Key words: myocardial infarction; pyruvate dehydrogenase; AMP-activated protein kinase.

Ischemic cardiomyopathy is a condition where the heart muscle is weakened and the left ventricle is usually enlarged and dilated. This condition can result from coronary artery stenosis or occlusion or chronic myocardial ischemia. Narrowing of the arteries prevents blood from reaching portions of the heart, whereas the weakened heart muscle inhibits the heart's ability to pump blood, potentially leading to heart failure (Bainey and Armstrong, 2014; Moussa and Li, 2012). Myocardial ischemia is currently a main cause of heart failure, associated with high mortality and morbidity worldwide (Bainey and Armstrong, 2014; Ma and Li, 2015; Morrison *et al.*, 2011). Myocardial ischemia is also a metabolic disease (Morrison and Li, 2011). Ischemia inhibits the oxidative metabolism of both free fatty acids and glucose due to the restriction of oxygen and nutrients; however, glucose transport and glycolytic ATP production are increased as an adaptation to the dramatic switch from aerobic to anaerobic metabolism (Young *et al.*, 1997). Several experimental and clinical studies have shown that a switch between fatty acid and glucose metabolism can be exploited for the treatment of myocardial ischemia (Anderson *et al.*, 2000; Costa *et al.*, 2012; Fragasso *et al.*, 2002; Lopaschuk, 1999; Louis *et al.*, 2002; Ma *et al.*, 2015; Wang *et al.*, 2013; Wolff *et al.*, 2002). Enhancing glucose oxidation can significantly reduce infarct size (Ma *et al.*, 2015; Ussher *et al.*, 2009; Wang *et al.*, 2013).

AMP-activated protein kinase (AMPK), a stress-activated protein kinase, plays a pivotal role in the intracellular adaptation to

energy stress during myocardial ischemia (Calvert *et al.*, 2008; Russell *et al.*, 2004; Wang *et al.*, 2011). The activation of AMPK during ischemia protects the myocardial tissues by decreasing cardiac infarct size, hypertrophy, apoptosis, and inflammation, and by limiting aggravation of the cardiac structure and function of the postischemic heart (Costa *et al.*, 2012; Ma *et al.*, 2010; Morrison *et al.*, 2011; Shibata *et al.*, 2005; Wang *et al.*, 2011). AMPK-deficient mice show significant aggravation of myocardial injury following ischemia (Miller *et al.*, 2008; Russell *et al.*, 2004). Some evidence indicates a strongly association between increased AMPK activities and increased glucose uptake (Costa *et al.*, 2012; Fraser *et al.*, 1999; Hayashi *et al.*, 2000; Ma *et al.*, 2015; Tian *et al.*, 2001).

The PDH complex is a multienzyme complex located in the mitochondrial matrix (Johnson *et al.*, 2001). It plays a key role in aerobic energy metabolism as a central crossroad between glycolysis and the tricarboxylic acid cycle by catalyzing the oxidative decarboxylation of pyruvate to form acetyl CoA (Reed, 1980). PDH complex consists of three catalytic components: pyruvate dehydrogenase (PDH) (E1), dihydrolipoamide acetyltransferase (E2), and dihydrolipoamide dehydrogenase (E3) (Patel and Roche, 1990). Enhancement of PDH activity by dichloroacetate (DCA, a PDH agonist) and subsequent glucose oxidation has been shown to decrease cardiac infarct size (Ussher *et al.*, 2009, 2012).

Both PDH and AMPK signaling pathway exert cardioprotective effects on the myocardium when it is subjected to stress. However, the mechanism by which PDH and AMPK activation modulate cardiac metabolism and execute cardioprotection remains elusive. The aims of the present study are to characterize the role of PDH and AMPK in eliciting cardioprotective effects against ischemic insults and to determine the relationship between PDH and AMPK activation in myocardial ischemic responses.

MATERIALS AND METHODS

Experimental animals

Wild-type (WT) male C57BL/6J mice and AMPK kinase dead (AMPK KD, α2 K45R mutation, driven in heart and skeletal muscles by the muscle creatine kinase promoter) mice (3–4 months) (Russell *et al.*, 2004) were used in these experiments. All animal protocols in this study were approved by the University of Mississippi Medical Center Institutional Animal Care and Use Committee.

Cardiac-specific deletion of the *Pdha1* gene was generated by breeding *PDH E1α*$^{flox/flox}$ mice (gifted from Mulchand S Patel, SUNY at Buffalo) (Johnson *et al.*, 2001). Females (genotype *PDHa1*^{flox8}/*PDHa1*^{flox8} with *Pdha1* ^{flox8} alleles having two loxP sites in the intronic sequences flanking exon 8) bred with transgenic male mice that carried an autosomally integrated *Cre* gene driven by the cardiac-specific alpha-myosin heavy chain promoter (αMHC) (Jackson Laboratory; 005657).

The genotyping of mice was performed in the following way: Genomic DNA was isolated with the Mouse Tail Quick Extraction kit (BioPioneer) either from tail or ear clips. The presence of *PDHa1* alleles (*PDHa1*^{wt}, *PDHa1*^{flox8}, and *PDHa1*$^{\Delta ex8}$) was determined by PCR analysis of the genomic DNA and the specific sets of primers. The inducible cardiac-specific PDH E1α knockout (CreER^{T2}-PDH$^{flox/flox}$) mice were generated by Tamoxifen (TM) injection (0.08 mg/g, ip 5 days) of CreER^{T2}-PDH$^{flox/flox}$ (12 weeks old) mice, and CreER^{T2} mice (12 weeks old) with TM injection were used for control groups.

In vivo regional ischemia and myocardial infarct size measurements

CreER^{T2}-PDH$^{flox/flox}$ mice and CreER^{T2}control mice were anesthetized with isoflurane and kept ventilated (Harvard Rodent Ventilator; Harvard Apparatus, Holliston, MA) during surgeries. The body temperature was maintained at 37 °C with a heating pad. After left lateral thoracotomy, the left anterior descending coronary artery (LAD) was occluded for 10 min or 24 h with an 8-0 nylon suture and polyethylene tubing to prevent arterial injury. An ECG and blanching of the left ventricle confirmed ischemic repolarization changes (ST-segment elevation) during coronary occlusion. After 10 min of ischemia, the hearts were excised and the ischemic region of the left ventricle was separated before freeze clamping in liquid nitrogen. Freeze-clamped heart tissues were stored at −80 °C until further immunoblotting analysis. Infarct sizes were measured by placing the hearts under ischemia for 24 h, followed by excision and staining with 2, 3, 5-triphenyltetrazolium at 37 °C. Nonnecrotic tissue in the ischemic region stained red, and slices were left in 10% formaldehyde overnight. The heart tissues then were fixed and sectioned into 1-mm slices, photographed with a Leica MZ95 microscope, and analyzed using NIH Image J software (U.S. National Institutes of Health, Bethesda, MD) (Morrison *et al.*, 2015; Tong *et al.*, 2013; Wang *et al.*, 2013). The myocardial infarct size was calculated as the area of myocardial necrosis as a percentage of the whole area of myocardium. DCA (50 mg/kg/day, Sigma, St. Louis, MO), a PDH agonist (Stacpoole and Greene, 1992; Ussher *et al.*, 2012), was administered to WT and CreER^{T2}-PDH$^{flox/flox}$ mice via intraperitoneal injection for 3 days before ligation of left anterior descending coronary artery.

Echocardiography

Transthoracic echocardiography was performed on mice at rest, following anesthesia with 1.5%–2.0% isoflurane, using a high-resolution imaging system for small animals (14.0 MHz, Sequoia 512; Acuson, München, Germany), equipped with a high-frequency ultrasound probe (GE-i13L). All hair was removed from the chest with a chemical hair remover. Parasternal long-axis and short-axis views were acquired. The left ventricular (LV) dimensions and wall thicknesses were determined from parasternal short axis M-mode images. The LV fractional shortening (FS) and LV ejection fraction (EF) were calculated as follows: FS (%) = [(LVIDd − LVAWd)/LVIDd] × 100; EF (%) = [(LVIDd3 − LVAWd3)/LVIDd3] × 100 (Din *et al.*, 2014; Liu *et al.*, 2014).

PDH activity measurements

PDH activity was determined with a Pyruvate Dehydrogenase Activity Assay Kit following the manufacturer's instructions (Sigma). The PDH activity was determined using a coupled enzyme reaction, which resulted in colorimetric (450 nm) product proportional to the enzymatic activity present. One unit of PDH is the amount of enzyme that will generate 1.0 μmol of NADH per minute at 37 °C.

Histological and immunohistochemical analysis

Hearts from WT and transgenic mice were collected at the indicated times, fixed overnight in 10% formalin, and embedded in paraffin. Serial 5-μm heart sections from each group were analyzed. Samples were stained with H&E for routine histologic examination, with Masson's trichrome for collagen, and with a wheat germ agglutinin-TRITC conjugate to identify

sarcolemmal membranes so that myofiber diameters could be quantified. Immunohistochemical staining was performed as described previously (Yang *et al.*, 2012; Zhang *et al.*, 2011b). The histological sections were localized in the area at risk and stained with primary antibodies against Mac-2 (1:200, Abcam) at 4 °C overnight. The bound antibodies were labeled using a second antibody (Vectastain ABC Kit, VECTOR Laboratories, Inc., Burlingame, CA). Peroxidase activity was visualized with diaminobenzidine, and the sections were counterstained with hematoxylin. Images were captured using a Zeiss Axioimager Motorized fluorescence microscope (Carl Zeiss, Oberkochen, Germany) and analyzed with NIH Image J software. The numbers of Mac-2 positive macrophages were counted blindly and expressed as a percentage of the total number of cardiomyocytes in five sequentially cut 5-μm sections of the ischemic lesion from each heart.

Immunoblotting and immunoprecipitation

Protein samples were prepared from hearts using lysis buffer (20 mM Tris-HCl [pH 7.5], 137 mM NaCl, 0.5% NP-40, 0.5 mM 1,4-Dithiothreitol (DTT), Complete Protease Inhibitor Cocktail [Roche, Mannheim, Germany], and Phosphatase Inhibitor Cocktail [Sigma]). Immunoblots and immunoprecipitations were performed as previously described (Ma *et al.*, 2010; Tong *et al.*, 2013). Protein concentrations were measured using a Bradford assay kit (Bio-Rad, Hercules, CA). The proteins were separated by 10% SDS-PAGE and then transferred to nitrocellulose membranes (Bio-Rad). The membranes were incubated with primary antibodies against phosphor-AMPK (Thr^{172}), AMPKα, PDHα, glyceraldehyde 3-phosphate dehydrogenase, and liver kinase B1 (LKB1) (obtained from Cell Signaling, Danvers, MA). Rabbit Sesn2 antibody was obtained from ProteinTech (Chicago, IL). Goat LKB1 antibody (M-18) was obtained from Santa Cruz Biotechnology (Santa Cruz, CA). Mice PDH E2/E3 antibody was obtained from Abcam (MitoSciences-Abcam, Eugene, OR). Horseradish peroxidase-conjugated secondary antibodies were obtained from Cell Signaling.

Quantitative real-time RT-PCR

Quantitative RT-PCR (Q-PCR) analysis was performed as described previously (Yang *et al.*, 2012). Total RNA was extracted using the RNeasy Mini Kit (Qiagen, Valencia, CA) according to the manufacturer's protocol. RNA samples (1 μg) were reverse-transcribed to generate first-strand cDNA. Q-PCR was performed in a 20 μl reaction mixture prepared with SYBR GREEN PCR Master Mix (Applied Biosystems, Warrington, UK) containing an appropriately diluted cDNA solution and 0.2 mM of each primer. The program consisted of 95 °C for 10 min, followed by 35 cycles at 95 °C for 10 s and 60 °C for 45 s. The transcript levels of IL-6, MMP-9, and Collagen I were detected by quantitative real-time polymerase chain reaction analysis using a real time-PCR system (Bio Rad CFX96 Touch PCR, Hercules, CA). All reactions were conducted in triplicate and the data were analyzed using the delta Ct (DDCt) method. These transcripts were normalized to β-actin.

Isolated heart perfusion for glycolysis and glucose uptake analysis

Glycolysis or glucose uptake was analyzed in the Langendorff heart perfusion system by measuring the production of ^3H_2O from D-[5-^{3}H]-glucose or D-[2-^{3}H]-glucose, respectively. Mice were heparinized (100 units) 10 min before anesthesia with isoflurane, and hearts were subsequently excised and perfused in a Langendorff mode with Krebs-Henseleit buffer (KHB) containing 7 mM glucose, 0.4 mM oleate, 1% bovine serum albumin, and 10 mU/ml insulin. Glycolysis or glucose uptake rate was determined simultaneously by the addition of D-[5-^{3}H]-glucose or D-[2-^{3}H]-glucose to the recirculating perfusate (Perkin Elmer, Waltham, MA). After addition of radioactive substrates, perfusion was continued under conditions of moderate cardiac work for 20 min, hearts were perfused for 20 min at a flow of 4 ml/min, followed by 10 min of global no-flow ischemia, and 20 min of reperfusion. Perfusate was recycled and collected every 5 min to test for radioactivity. Metabolized ^3H_2O was separated from D-[5-^{3}H]-glucose or D-[2-^{3}H]-glucose by filtering through Dowex columns (3 ml bed volume of AG 1-×8 Resin, Bio-Rad) extensively washed with distilled H_2O after pretreatment with 1 N NaOH. The PDH agonist treatment group was administered DCA at a 1.5 mM final concentration prior to heart perfusion.

Cell surface GLUT4 labeling

To distinguish cell surface and intracellular GLUT4, cell membrane GLUT4 labeling with 4,4′-O-[2-[2-[2-[2-[2-[6-(biotinylamino)hexanoyl]-amino]ethoxy]ethoxy]-ethoxy]-4-(1-azi-2,2,2,-trifluoroethyl)benzoyl]amino-1,3-propanediyl]bis-D-glucose (bio-LC-ATB-BGPA) was performed as described (Miller *et al.*, 2007). After perfusion, mouse hearts were flushed through aortic cannulation with 1 ml ice-cold glucose-free KHB and then perfused with KHB containing 300 μM bio-LC-ATB-BGPA. After infused with bio-LC-ATB-BGPA, hearts were incubated at 4 °C for 15 min. In order to enhance crosslink between bio-LC-ATB-BGPA and cell surface GLUT4, the left ventricle (LV) and right ventricle were cut sagittal and reactions were exposed to UV irradiation on both sides for 5 min each. Heart tissues were then freeze-clamped and stored in −80 °C. To isolate cell surface GLUT4 protein, the photolabeled heart tissues were homogenized in 500 μl of HEPES-EDTA-sucrose buffer containing 20 mM 4-(2-Hydroxyethyl) piperazine-1-ethanesulfonic acid (HEPES), 5 mM Na-EDTA, 255 mM sucrose, and protease inhibitor cocktail (Hoffmann-La Roche Inc., Indianapolis, IN). Tissue homogenates were centrifuged at 20 000g at 4 °C for 15 min and pellets were discarded. To isolate the photolabeled GLUT4, 400 μg total membrane protein was incubated with 100 μl streptavidin bound to 6% agarose beads (Pierce, Rockford, IL) at 4 °C overnight. The steptavidin-agarose isolated labeled fraction of GLUT4 was washed extensively with PBS containing decreasing concentrations of Thesit (1, 0.1, and 0%). The labeled GLUT4 was then dissociated from streptavidin by boiling in the loading buffer for 30 min prior to analysis by SDS-PAGE.

Fatty acid/glucose oxidation analysis

An *ex vivo* working heart system was used to determine the metabolism of fatty acid and glucose (Kantor *et al.*, 2000). Isolated mouse hearts were subjected to retrograde perfusion with KHB containing 7 mM glucose, 0.4 mM oleate, 1% bovine serum albumin (BSA) and a low fasting concentration of insulin (10 μU/ml). Hearts were perfused for 20 min at a flow of 4 ml/min, followed by 10 min of global no-flow ischemia, and 20 min of reperfusion. Mice were given 100 units of heparin (ip, Sagent Pharmaceuticals, Schaumburg, IL) 10 min before anesthesia. Oxidation rates were determined at 5-min intervals and are expressed as micromoles of fuel oxidized per minute per gram dry heart weight. Glucose and oleate oxidation rates were determined simultaneously by the quantitative collection of ^3H_2O

and $^{14}CO_2$ produced by hearts perfused with buffer containing U-^{14}C-glucose (20 μCi/l) and [9, 10]-^{3}H-oleate (50 μCi/l) (both isotopes from Perkin Elmer). The rate of glucose oxidation was calculated by the amount of $^{14}CO_2$ appearing in the effluent gas and buffer. Aliquots from the 1 N NaOH gas traps were placed directly into scintillation vials and measured. The$^{14}CO_2$ present as bicarbonate was determined by syringe removal of an aliquot of the perfusate buffer while avoiding exposure to air. Oleic acid oxidation was measured simultaneously as the rate of appearance of $^{3}H_2O$ in the perfusate. Tritiated $^{3}H_2O$ was separated from [9, 10]-^{3}H-oleate by filtering samples (0.4 ml) through Dowex-1-borate columns [3 ml bed volume of AG 1-×2 Resin (106–250 μm mesh) (Bio-Rad)], followed by extensive washing with distilled H_2O. The DCA treatment group was administered DCA at a 1.5 mM final concentration prior to heart perfusion.

Statistical analysis

Data were collected from experimental animals (n = 4–7 per group) and presented as means ± SEM, as indicated, using Image GraphPad Prism 5.0 software (GraphPad Software, La Jolla, CA) for analysis. Comparisons were performed using either a two-tailed, unpaired Student's *t* test or ANOVA using Tukey's posttest. A value of $P < .05$ was considered statistically significant.

RESULTS

Cardiac hypertrophy, fibrosis, inflammation and contractile dysfunction in the CreER^{T2}-PDH$^{flox/Flox}$ mice

To examine the pathophysiological roles of PDH E1α deficiency in heart, we generated the α-MHC-MerCreMer mice on the genetic background of PDHa1$^{flox/flox}$ (CreER^{T2}-PDH$^{flox/flox}$) and those on α-MHC-MerCreMer/PDHa1 as a control (CreER^{T2}). The genotyping of control (CreER^{T2}) and CreER^{T2}-PDH$^{flox/flox}$ was determined by PCR analysis (Figure 1A). *Pdha1* gene is located in X chromosome, thus there is only one product shown in CreER^{T2}-PDH$^{flox/flox}$ (male) but two products in the CreER^{T2}-PDH$^{flox/flox}$ (female) (Figure 1A right panel). The levels of PDH E1α in mouse hearts were verified by immunoblotting (Figure 1B). The PDH E1α protein level was markedly reduced in the adult mouse heart 2 months after TM injection for 5 days (Figure 1B). In these mice, PDH E1α deficiency was only occurred in the heart (Figure 1C) and these inducible cardiac PDH-deficient mice versus control were used in all experiments.

The CreER^{T2}-PDH$^{flox/flox}$ mice demonstrated high mortality rate as shown in Figure 2A. We next examined whether *Pdha1* gene ablation results in cardiac dysfunction. At 12–16 weeks of age, the heart weight-to-body weight ratio was significantly increased in CreER^{T2}-PDH$^{flox/flox}$ mice compared with CreER^{T2} control mice (Figure 2B). Histological evaluation using a wheat germ agglutinin-TRITC conjugate showed significantly larger (2.1-fold) ventricular cardiomyocytes in CreER^{T2}-PDH$^{flox/flox}$ mice than that in CreER^{T2} control mice (Figure 2B, second panel). The effect of PDH E1α deficiency on cardiac inflammation was assessed by the immunohistochemical staining with antibody against Mac-2 (a marker for macrophages). More inflammatory cells had infiltrated the hearts of CreER^{T2}-PDH$^{flox/flox}$ mice, the number of Mac-2-positive cells was increased 11.4-fold as compared with the CreER^{T2} control mouse hearts (Figure 2B, third panel). The heart sections were stained with Masson's trichrome to show cardiac fibrosis, the results demonstrated that a 25.7% increase in fibrosis in the CreER^{T2}-PDH$^{flox/flox}$ hearts when compared with CreER^{T2} control hearts (Figure 2B, fourth panel).

The effect of cardiac PDH E1α deficiency on cardiac function was determined by echocardiography in terms of the cardiac performance parameters (Figure 2C and Table 1). Consistent with cardiac fibrosis, PDH E1α deficiency accelerated the cardiac dysfunction. The left ventricle interior diameter during diastole (LVIDd) was increased 33.5%, meanwhile EF was decreased in CreER^{T2}-PDH$^{flox/flox}$ hearts as compared with CreER^{T2} control hearts (Figure 2C)

Q-PCR analyses showed that mRNA expression of MMP-9 (profibrotic gene) and remodeling related gene Collagen I were markedly upregulation in CreER^{T2}-PDH$^{flox/flox}$ hearts when compared with CreER^{T2} control hearts (Figure 2D). The inflammation-related cytokine IL-6 was also significantly upregulated in cardiac PDH E1α-deficient heart (Figure 2D). In conclusion, PDH E1α deficiency in heart caused an aggravation of cardiomyocyte hypertrophy, inflammation, and fibrosis.

Decreased glucose oxidation in the CreER^{T2}-PDH$^{flox/Flox}$ mouse hearts

The *ex vivo* working heart system model was used to determine the differences between CreER^{T2}-PDH$^{flox/flox}$ and CreER^{T2} control mouse hearts in substrate metabolism. The results demonstrated that PDH E1α deficiency significantly decreased glucose oxidation but not affect oleate oxidation under normal physiological condition (Figure 2E). Moreover, PDH E1α deficiency did not affect glycolysis in the heart under normal physiological condition (Figure 2E).

Cardiac-specific PDH E1α deficiency increased susceptibility to ischemic injury

To further explore the biological consequence of cardiac PDH E1α deficiency specifically in ischemic heart, *in vivo* regional ischemia was generated in CreER^{T2}-PDH$^{flox/flox}$ and CreER^{T2} control mice. In CreER^{T2} control mouse hearts, 24 h of LAD ligation (ischemia) significantly reduced myocardial PDH activity versus basal condition (Figure 3A) and the LAD ligation for 24 h resulted in myocardial infarction in CreER^{T2} control hearts (44% of myocardium; Figure 3B). Furthermore, the CreER^{T2}-PDH$^{flox/flox}$ hearts demonstrated dramatically low PDH activity versus CreER^{T2} control hearts under both basal and ischemia conditions (Figure 3A), and there is a larger myocardial infarction in CreER^{T2}-PDH$^{flox/flox}$ hearts as compared with CreER^{T2} control hearts (Figure 3B).

The importance of PDH activation in cardioprotection against ischemic injury was determined by adding DCA, a PDH activator through inhibiting PDH kinase (Bersin and Stacpoole, 1997). Injection with DCA (50 mg/kg/day ip) significantly increased the myocardial PDH activity under both basal and ischemia conditions when compared with mice injected with vehicle alone in the CreER^{T2} control mice but there is no any effect in CreER^{T2}-PDH$^{flox/flox}$ mice (Figure 3A). The DCA treatment significantly reduced myocardial infarction size in CreER^{T2} control hearts but not in CreER^{T2}-PDH$^{flox/flox}$ hearts (Figure 3B). The immunohistochemical staining showed that DCA as a PDH agonist significantly inhibited the cardiac fibrosis caused by myocardial ischemia (Figure 3C). Masson's trichrome staining of hearts showed that DCA treatment decreased fibrosis by 42% versus vehicle in CreER^{T2} control hearts (Figure 3C). Mac-2 staining to assess the extent of inflammation, the results

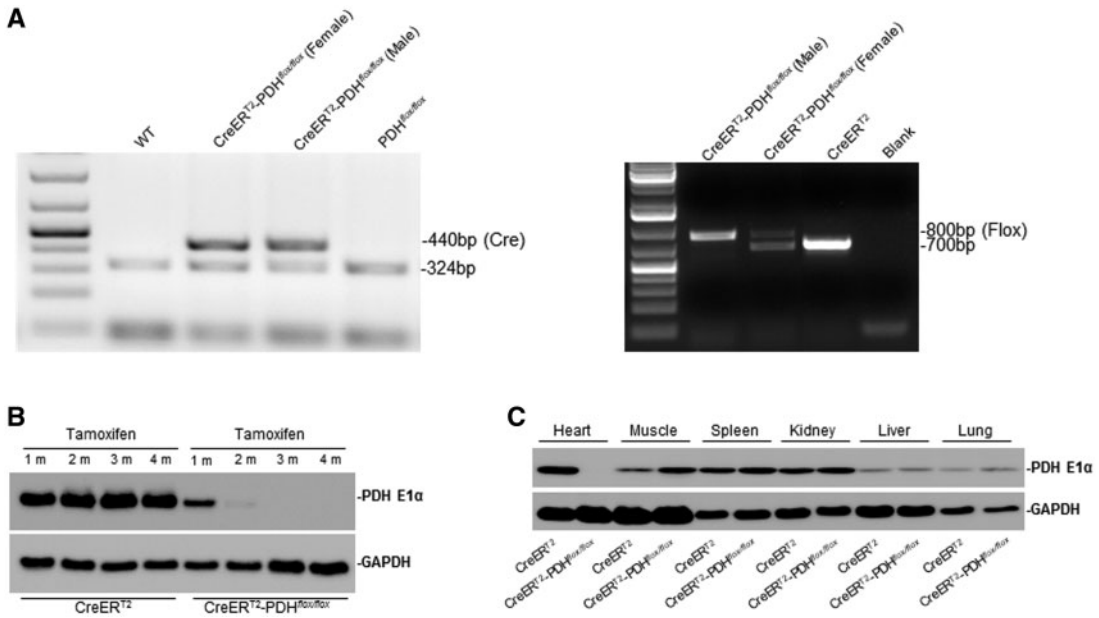

FIG. 1. Cardiac-specific PDH E1α deficiency mice. A, Genotyping of CreER^{T2}-PDH$^{flox/flox}$ and CreER^{T2}(α-MHC-MerCreMer) mice by PCR analysis. B, Immunoblotting verified the level of PDH E1α in heart. The PDH E1α protein level was markedly reduced in the adult mouse heart 2 months after tamoxifen (TM) injection for 5 days. C, The immunoblotting shows the PDH E1α was specifically knock out in the adult mouse heart after TM injection.

demonstrated that there is a 49% decrease in the amount of Mac-2 positive cells in hearts of DCA-treated mice (Figure 3C).

Activation of PDH by DCA modulates glucose and fatty acid oxidation

We have observed the impaired cardiac glucose oxidation in CreER^{T2}-PDH$^{flox/flox}$ hearts (Figure 2E). To provide further support for the hypothesis that PDH activation by DCA leads to a cardioprotective effect against ischemic insults, an *ex vivo* working heart perfusion system was used to determine the metabolism of fatty acid and glucose. The working heart results showed PDH agonist DCA treatment of CreER^{T2} control heart accelerated GLUT4's translocation to cell surface during ischemia (Figure 4A), the DCA treatment also significantly augmented glucose uptake (Figure 4B) and glycolysis level (Figure 4C) during ischemia and reperfusion (I/R). Accordingly, DCA treatment significantly shifted the increased oleate oxidation in favor of increased glucose oxidation during I/R (Figure 4D). These results suggest that PDH activation by DCA significantly modulates the substrate metabolism in hearts during I/R.

AMPK mediates the cardioprotection of DCA

Accumulating evidence suggests that AMPK is a "metabolic modulator" that could be an important effector of the switch between fatty acid and glucose oxidation during ischemic injury (Costa *et al.*, 2012; Hardie and Hawley, 2001; Ma *et al.*, 2015; Winder and Hardie, 1999). We and others have shown that AMPK activation can improve the energetics during ischemia (Marsin *et al.*, 2000; Morrison *et al.*, 2015; Wang *et al.*, 2013), leading to rapid changes in fatty acid and glucose oxidation by increasing glucose uptake (Costa *et al.*, 2012; Ma *et al.*, 2015) and rates of glycolysis and ATP generation (Marsin *et al.*, 2000). PDH is also a metabolism-related protein that protects against ischemic injury, our results showed the metabolic-shift function after PDH activation by DCA (Figure 4). Thus, we hypothesized that PDH might modulate AMPK activation, thereby promoting cardioprotection. Immunoblotting analysis of myocardial lysates taken from ischemic injury area demonstrated that ischemia-induced AMPK phosphorylation was significantly attenuated in CreER^{T2}-PDH$^{flox/flox}$ hearts versus CreER^{T2} control heart (Figure 5A).

Furthermore, in order to characterize the role of AMPK in the cardioprotection of PDH against ischemic damage, we examined the effect of PDH agonist DCA treatment on the myocardial infarction of WT and AMPK KD transgenic mice with ligation of left anterior descending coronary artery for 24 h, the results showed that DCA treatment significantly reduced myocardial infarct size in WT hearts but not in AMPK KD hearts (Figure 5B). Moreover, the *ex vivo* working heart perfusion experiments demonstrated that DCA administration significantly increased glucose oxidation in WT heart during I/R, but did not have any effect in AMPK KD heart (Figure 5C). Interestingly, DCA administration inhibited oleate oxidation in both WT and AMPK KD hearts during I/R (Figure 5D). The results suggest that PDH agonist DCA administration modulates glucose oxidation in the heart via AMPK signaling pathway, but the effect of oleate oxidation by DCA is not associated with the AMPK signaling pathway.

Cardiac-specific PDH E1α deficiency alters LKB1-Sestrin2 interaction

Our results showed that PDH activation modulates ischemia-induced AMPK signaling pathway. We used immunoblotting to analyze the changes in the AMPK upstream kinases and the activities of AMPK-associated phosphatases during ischemia. The results demonstrated that AMPK upstream LKB1 and calmodulin-dependent protein kinase kinase β (Moussa and Li, 2012), and phosphatases PP2A and PP2C (Morrison and Li, 2011) did not show any difference in WT and PDH-deficient hearts under both basal and ischemia conditions (data not shown). Recently, we identified a novel scaffold protein Sestrin2 that modulates cardiac AMPK activation via AMPK upstream LKB1 in response to

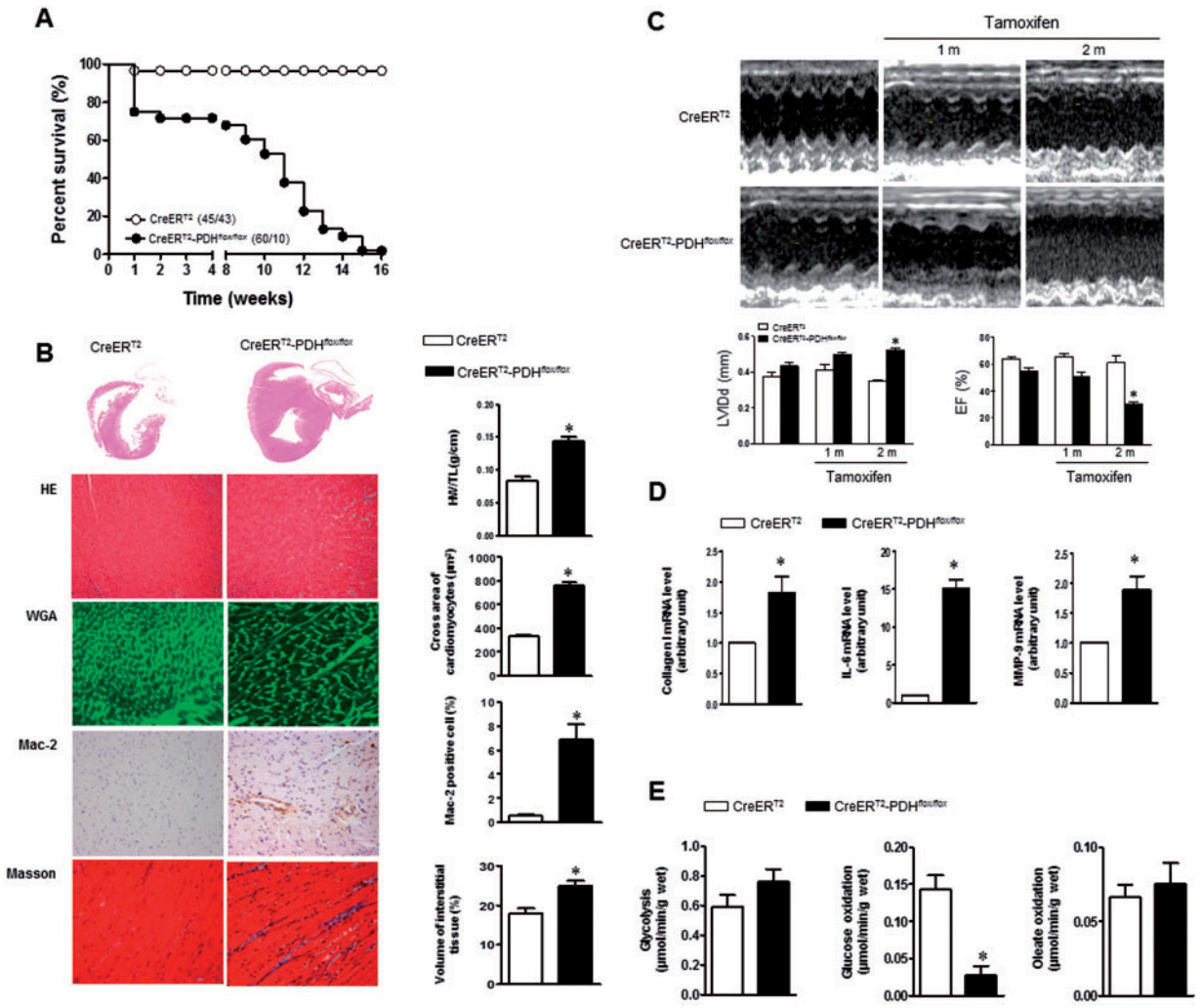

FIG. 2. Cardiac abnormalities in the PDH E1α iCKO mice. A, Survival analysis in PDH E1α-deficient (CreER^{T2}-PDH$^{flox/flox}$) and CreER^{T2} control mice. B, H&E staining of heart sections. The ratios of heart weight and body weight increased in PDH E1α-deficient (CreER^{T2}-PDH$^{flox/flox}$) mice when compared with CreER^{T2} control mice (upper panel). Wheat germ agglutinin (WGA) staining showed larger ventricular cardiomyocytes in cardiac PDH E1α-deficient heart than that in CreER^{T2} heart (the second panel). The expression of Mac-2 protein in the heart was identified by immunohistochemistry and quantified by positive staining of the cells (the third panel). Masson staining of heart sections showed the PDH E1α deficiency increased cardiac fibrosis (the fourth panel). C, Serial echocardiographic studies performed at baseline (before injection of tamoxifen), 1 month, and 2 months after tamoxifen injection. The bar graphs show the left ventricle inner diameter during diastole (LVIDd) and ejection fraction (EF). D, The mRNA levels of collagen I, IL-6 and MMP-9 in PDH E1α-deficient (CreER^{T2}-PDH$^{flox/flox}$) and CreER^{T2}control heart were analyzed by Q-PCR. E, Glucose/oleate oxidation ih the PDH E1α-deficient (CreER^{T2}-PDH$^{flox/flox}$) and CreER^{T2}control heart. Data are means ± SEM (n = 4–7 per group). *P < .05 versus CreER^{T2} control.

TABLE 1. Echocardiographic Assessment of Cardiac Function of WT (CreER^{T2}) and PDH E1α-Deficient (CreER^{T2}-PDH$^{flox/flox}$) Mice With Injection of Tamoxifen in Time-Dependent Manner

	CreER^{T2} (n = 4)			CreER^{T2}-PDH$^{flox/flox}$ (n = 4)		
	Tam 0 m	Tam 1 m	Tam 2 m	Tam 0 m	Tam 1 m	Tam 2 m
IVSd (mm)	0.60 ± 0.04	0.60 ± 0.10	0.80 ± 0.01	0.70 ± 0.08	0.60 ± 0.02	0.80 ± 0.01
LVIDd (mm)	3.70 ± 0.25	3.80 ± 0.22	3.50 ± 0.08	4.30 ± 0.19	4.90 ± 0.11	5.20 ± 0.01*
LVPWd (mm)	1.50 ± 0.08	1.00 ± 0.15	1.10 ± ± 0.27	1.20 ± 0.28	1.00 ± 0.18	1.20 ± 0.58
EF (%)	63.64 ± 2.02	65.77 ± 2.15	60.92 ± 4.93	54.56 ± 2.80	50.84 ± 3.33	29.92 ± 2.18*

Abbreviations: IVSd = interventricular septal end diastole, LVIDd = left ventricular internal diameter end diastole, LVPWd = left ventricular posterior wall end diastole, EF = ejection fraction

Values are means ± SEM.

*P < .05 versus CreER^{T2} Tam 2 m.

ischemic stress (Budanov and Karin, 2008; Morrison *et al.*, 2015). We examined whether residual PDH complex (E2/E3) after cardiac PDH E1α deficiency is involved in modulating Sestrin2-LKB1 complex that regulates cardiac AMPK activation during ischemia. The immunoprecipitation with Sestrin2 antibody demonstrated that cardiac PDH E1α deficiency results in more Sestrin2

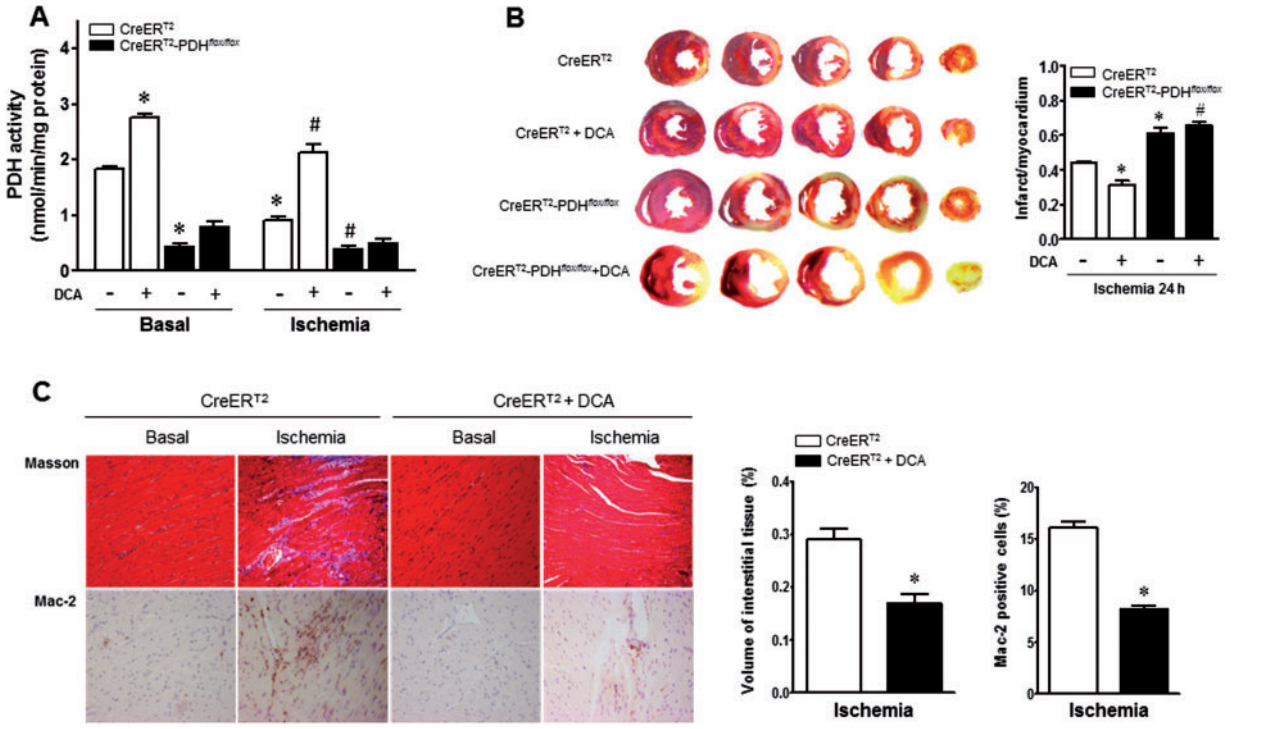

FIG. 3. Cardiac-specific PDH E1α deficiency increased susceptibility to ischemic injury. A, PDH activity was abolished in PDH E1α-deficient (CreER^{T2}-PDH$^{flox/flox}$) heart. There is reduction of PDH activity in CreER^{T2} heart during ischemia. Dichloroacetate (DCA) treatment increased PDH activity in CreER^{T2} heart under both basal and ischemic conditions. Values are means ± SEM (n = 4 per group). *$P < .05$ versus CreER^{T2} basal, #$P < .05$ versus CreER^{T2} ischemia alone. B, Cardic PDH E1α-deficient (CreER^{T2}-PDH$^{flox/flox}$) mice and CreERT2 control mice with and without DCA administration were subjected to *in vivo* regional ischemia for 24 h. DCA (50 mg/kg/day) was given for 3 days before myocardial ischemia by ligation of left anterior descending coronary artery (LAD). Representative sections are shown the extent of myocardial infarction. The ratios of the infarction area to the total heart are shown in the right bar graph. Values are means ± SEM (n = 4–6 per group). *$P < .05$ versus CreER^{T2} ischemia alone, #$P < .05$ versus CreER^{T2} ischemia + DCA. C, Masson trichrome stained to determine fibrosis and Mac-2 stained for inflammation measurement in 1 week after ischemia. Values are means ± SEM (n = 4 per group). *$P < .05$ versus CreER^{T2} ischemia alone.

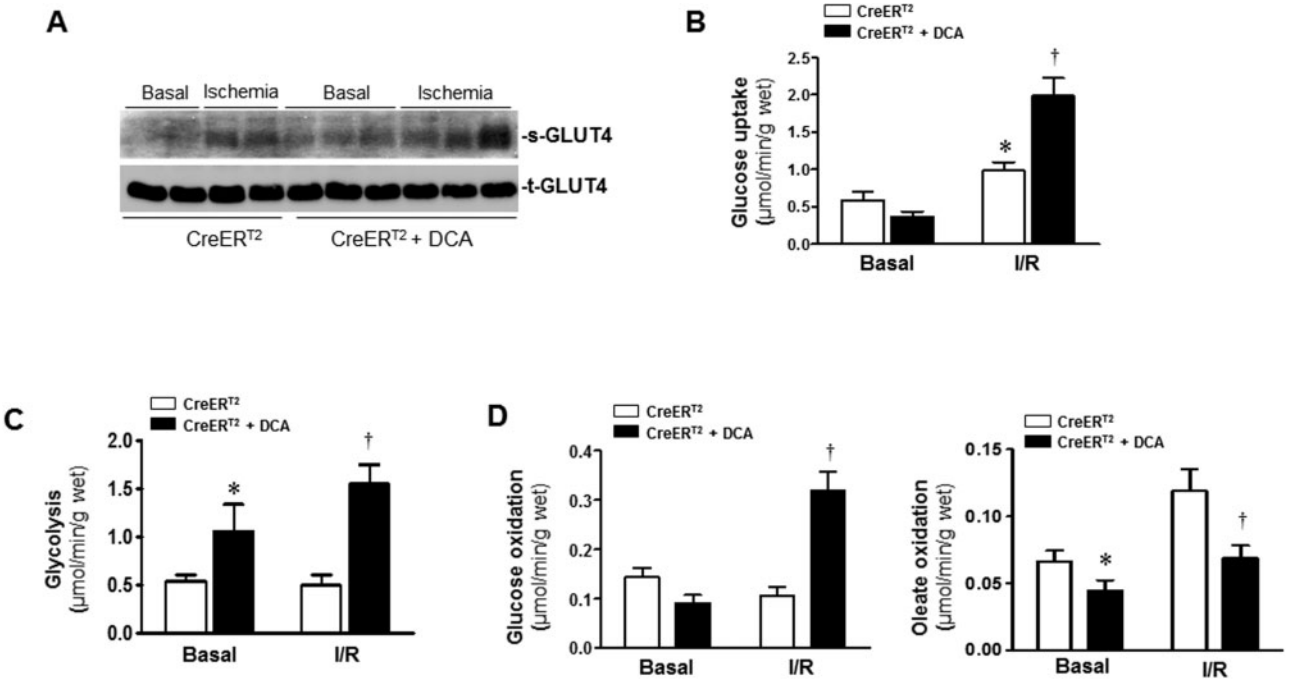

FIG. 4. Activation of PDH by DCA modulates glucose and fatty acid oxidation. A, DCA was given at the beginning of the perfusion, after balancing 20 min, isolated CreER^{T2} hearts were subjected to 10 min of ischemia for GLUT4 translocation measurement. After balancing 20 min, isolated CreER^{T2} hearts were subjected to 10 min of ischemia followed by 20 min of reperfusion for measurement of glucose uptake (B), glycolysis (C), and (D) glucose oxidation and oleate oxidation in the heart. Values are means ± SEM (n = 4–6 per group). *$P < .05$ versus CreER^{T2} basal, †$P < .05$ versus CreER^{T2} I/R alone.

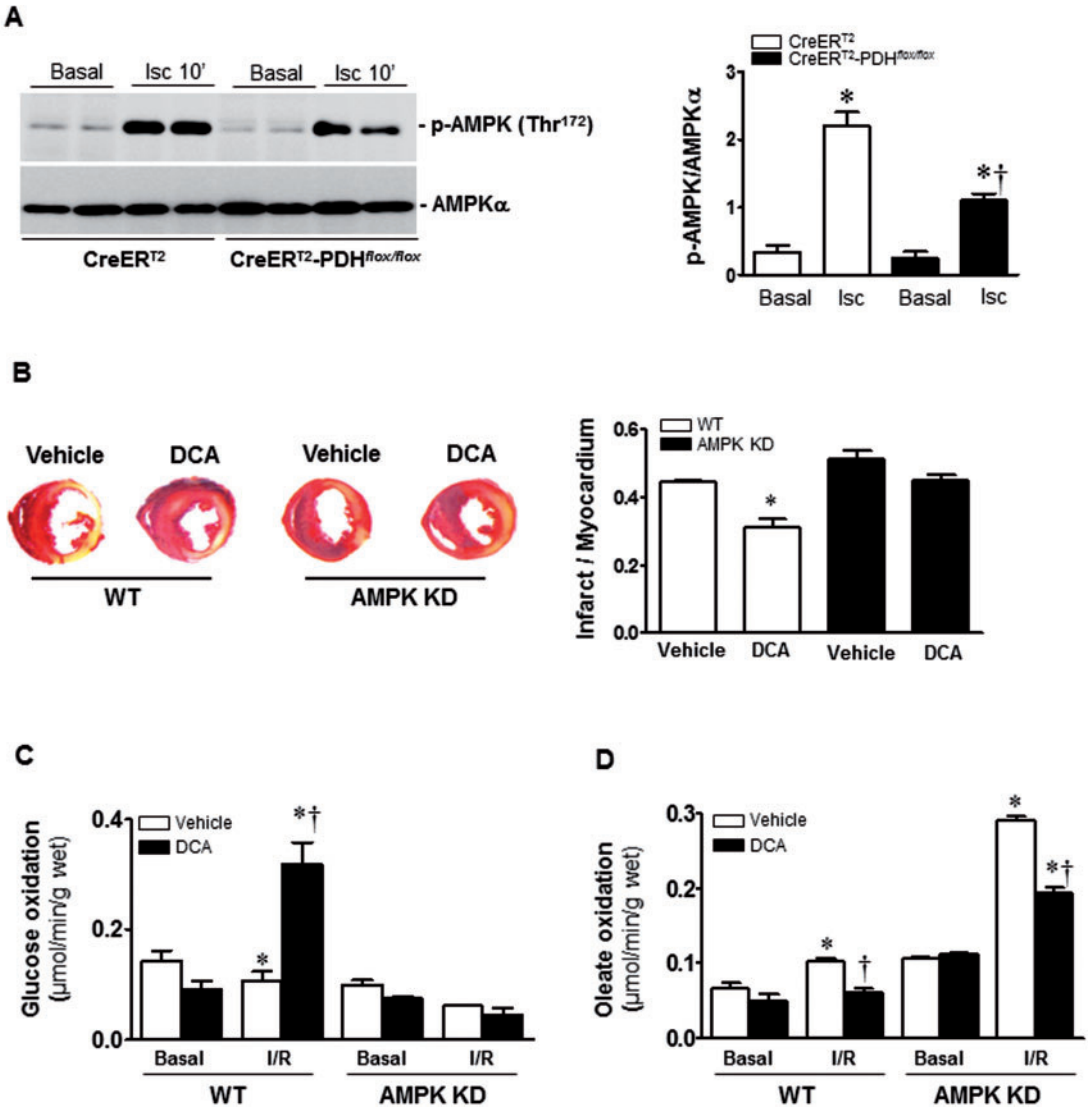

FIG. 5. AMPK mediates the cardioprotection of DCA. A, Cardic PDH E1α-deficient (CreER^{T2}-PDH$^{flox/flox}$) heart and CreER^{T2} control heart with or without DCA administration were subjected to ischemia 10 min by LAD ligation. The levels of phospho-AMPK and total AMPK in the heart were determined by immunoblotting. Values are means ± SEM (n = 3 per group). *$P < .05$ versus CreER^{T2} basal; †$P < .05$ versus CreER^{T2} ischemia. B, AMPK kinase-dead (AMPK KD) transgenic mice and wild type (WT) mice with or without dichloroacetate (DCA) treatment were subjected to *in vivo* regional ischemia for 24 h. Representative sections show the extent of myocardial infarction. The ratios of the infarction area to the total heart is shown in the bar graph. Values are means ± SEM (n = 4 per group). *$P < .05$ versus WT Vehicle. (C,D) AMPK KD transgenic hearts and WT hearts with or without DCA treatment were subjected to a working heart perfusion system to measure substrate metabolism. C, Glucose oxidation measurement with U-^{14}C-glucose (20 μCi/l). Values are means ± SEM (n = 4–6 per group). *$P < .05$ versus Basal vehicle; †$P < .05$ versus WT I/R. (D) Oleate oxidation measurement with [9, 10]-^{3}H-oleate (50 μCi/l). Values are means ± SEM (n = 4 per group). *$P < .05$ versus Basal vehicle, respectively; †$P < .05$ versus WT I/R vehicle or AMPK KD vehicle I/R, respectively.

combined with PDH E2 and E3 complex whereas inhibiting Sestrin2's interaction with LKB1 in CreER^{T2}-PDH$^{flox/flox}$ heart (Figure 6). These results support that cardiac-specific deletion of the *Pdha1* gene blunted Sestrin2's interaction with LKB1 contributes to the AMPK inactivation in CreER^{T2}-PDH$^{flox/flox}$ heart.

DISCUSSION

In the present study, using CreER^{T2}-PDH$^{flox/flox}$ mice, we evaluated the pathophysiological roles of PDH E1α deficiency in basal metabolism and myocardial anti-ischemic damage capability. Cardiac-specific PDH E1α deficiency led to cardiac hypertrophy, fibrosis, and inflammation phenotype accompanied with contractile dysfunction in the CreER^{T2}-PDH$^{flox/flox}$ mice. Glucose oxidation was impaired in CreER^{T2}-PDH$^{flox/flox}$ mice, it is concomitant with exaggerated ischemic injury. On the contrary, PDH activation by DCA leads to a cardioprotective effect against ischemic insults, DCA administration reduced myocardial infarction size, and inhibited the cardiac fibrosis caused by myocardial ischemia and decrease Mac-2 positive cells in the ischemic hearts. More importantly, the activation of PDH by DCA significantly enhanced GLUT4's translocation to cell surface and augmented glucose uptake. Hence, DCA treatment significantly shifted the increased oleate oxidation in favor of increased glucose oxidation during I/R that benefits the hearts under ischemic conditions. Moreover, PDH activation by DCA-induced metabolic-shift function was mediated by AMPK signaling pathway. Furthermore, we found that PDH E1α deficiency

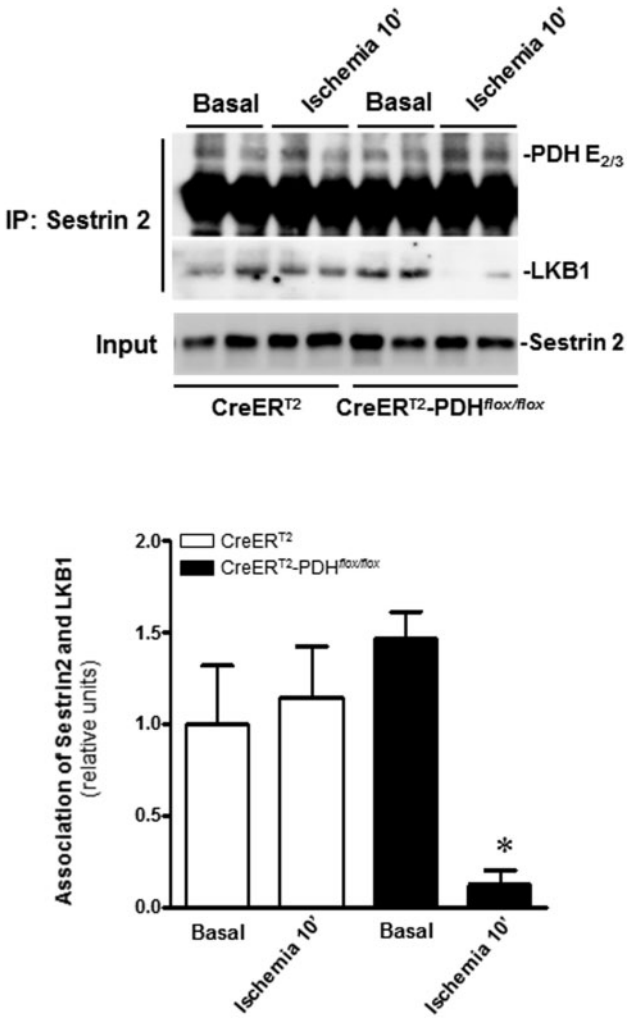

FIG. 6. Cardiac-specific PDH E1α deficiency alters LKB1-Sestrin2 interaction. Immunoprecipitation was performed using anti-Sestrin2 antibody. The precipitates were analyzed by Western blotting with antibodies recognized against PDH E2/3 and LKB1, respectively. Values are means ± SEM (n = 4 per group). *P < .05 versus CreER^{T2}-PDH$^{flox/flox}$ Basal.

could lead to PDH E2/E3 stay outside of mitochondria that result in the interaction between Sestrin2 and PDH E2/E3 in the PDH E1α-deficient heart, which may be a feasible mechanism of AMPK inactivation in ischemic CreER^{T2}-PDH$^{flox/flox}$ heart and ultimately reduce the resistance to ischemic injury. Collectively, intrinsic activity of PDH is required for the modulation of myocardium energy metabolism to limit cardiac damage during I/R.

The protective role for PDH in controlling substrate metabolism during I/R has been attracted attentions (Katayama *et al.*, 1998). The present study demonstrated that the cardioprotective role of PDH against ischemic injury through modulation of glucose metabolism and cardiac AMPK signaling pathway. The underlying mechanism for regulation of the PDH-AMPK signaling cascades is mediated by the LKB1-Sestrin2 complex that has been identified for modulating AMPK activation by our group in the ischemic heart (Morrison *et al.*, 2015), and AMPK signaling is impaired in the PDH E1α deficiency heart that could be responsible for the more susceptibility of PDH-deficient heart to ischemic insults. There is evidence that the cardioprotective effects of PDH against myocardial infarction are at least partially mediated by AMPK pathway. The AMPK signaling pathway is a well-known critical energy sensor in the ischemic heart to protect heart from myocardial infarction and heart failure (Ceylan-Isik *et al.*, 2010; Morrison and Li, 2011; Russell *et al.*, 2004). Our previous studies using genetic mouse models with impaired cardiac AMPK activation showed increased injury during I/R (Ma *et al.*, 2010; Miller *et al.*, 2008; Russell *et al.*, 2004; Wang *et al.*, 2013). AMPK activation may directly alter cell survival by regulating apoptosis, autophagy, endoplasmic reticulum stress, and the generation of reactive oxygen species (ROS) (Ma and Li, 2015; Ma *et al.*, 2015; Morrison and Li, 2011). In the present study, activation of PDH by DCA significantly lead to a decrease in the infarct size in WT mice, but no significant differences were observed in AMPK KD mice. Therefore, cardiac AMPK signaling pathway plays an important role in DCA's cardioprotection against myocardial infarction via activation of PDH.

The control of PDH activity is an essential part of the overall control of glucose metabolism. Under normal physiological conditions, glucose metabolism and fatty acid metabolism proceed together to provide ATP for keep heart's contractile functions (Morrison and Li, 2011; Taegtmeyer *et al.*, 2004). In situations of ischemia, the metabolic shifts occur in the heart, including the regulation of fatty acid and glucose oxidation and glycolysis. Anaerobic glycolysis becomes a more important source of energy. However, insufficient ATP is generated by glycolysis, so free fatty acid oxidation becomes the major oxidative pathway (Ma and Li, 2015; Morrison and Li, 2011). The high rate of fatty acid oxidation produces high levels of acetyl-coenzyme A, which negatively feeds back on PDH activity and inhibits glycolysis. In the present study, PDH E1α-deficient hearts showed a clear decrease in glucose oxidation in the normal physiological condition. However, stimulation of PDH activity by DCA can significantly increase glucose oxidation and inhibit fatty acid oxidation in the heart during I/R that benefits the heart via reduction of ROS generation during I/R (Ma and Li, 2015).

The harm induced by increasing fatty acid oxidation can be associated with in an influx of oxygen levels that lead to more ROS generated from mitochondria, resulting in cardiomyocyte damage (Costa *et al.*, 2012; Ma and Li, 2015; Ma *et al.*, 2015). An interesting observation in the present study was that glucose oxidation was augmented in WT heart but not in AMPK KD heart by PDH agonist DCA during I/R condition, it suggests that AMPK plays a critical role in PDH modulating cardiac glucose oxidation during I/R. There is a big increase in oleate oxidation in AMPK KD heart during I/R that could be reason for the more susceptibility of AMPK KD heart to ischemic insults (Russell *et al.*, 2004; Wang *et al.*, 2013). Intriguingly, PDH activation by DCA significantly reduced oleate oxidation in AMPK KD heart during I/R that could inhibit ROS generation from I/R AMPK KD heart.

The AMPK upstream kinase LKB1 plays an important role in glucose homeostasis (Sakamoto *et al.*, 2006) that is associated with regulating AMPK signaling pathway (Ma *et al.*, 2010; Morrison *et al.*, 2015; Morrison and Li, 2011). The scaffold protein Sestrin2 is a stress inducible protein, which is targeted by hypoxia inducible factor-1α during ischemia (Zhang *et al.*, 2011a). Recently, we have showed that Sestrin2 forms a complex with AMPK upstream LKB1 that modulates cardiac AMPK activation (Morrison *et al.*, 2015); moreover, the interaction between LKB1 and Sestrin2 was strengthened during ischemia (Morrison *et al.*, 2015). Interestingly, the immunoprecipitation of Sestrin2 demonstrated that Sestrin2-LKB1 complex also interacts with PDH complex. The cardiac PDH E1α deficiency significantly decreases the association between Sestrin2 and LKB1; therefore, there is a significantly impaired AMPK activation in PDH E1α-deficient heart in response to ischemic stress. In present study, it should be noted that PDH E1α

knockout could lead to PDH E2 and E3 stay outside of mitochondria that result in the interaction between Sestrin2 and PDH E2/E3 in the PDH-deficient heart. We will address the detailed mechanism of this interaction in the future studies.

CONCLUSIONS

A novel evidence is presented to show that activation of PDH can modulate energy metabolism to alleviate the cardiac damage caused by I/R. In addition, the cardioprotective effect of PDH is associated with activation of the AMPK signaling pathway, through modulation of the interaction between Sestrin2 and LKB1 in response to ischemic insults. Collectively, these findings suggest a mechanism for cardioprotection by PDH against myocardial infarction, and shed light on potential new strategies for prevention of ischemic heart disease.

ACKNOWLEDGMENT

The authors thank Dr Mulchand S. Patel from State University of New York at Buffalo, who provided the *PDH E1α*$^{flox/flox}$ mice. They declare that they have no conflict of interest.

FUNDING

American Heart Association (14IRG18290014); American Diabetes Association (1-14-BS-131); the National Institutes of Health (R21AG044820, P01HL051971, P20GM104357 and R01AG049835); National Natural Science Foundation of China (81471394 and 81500264).

REFERENCES

Anderson, J., Khou, S., and Nawarskas, J. (2000). Ranolazine: A potential new treatment for chronic stable angina. *Heart Dis.* **3**, 263–269.

Bainey, K. R., and Armstrong, P. W. (2014). Clinical perspectives on reperfusion injury in acute myocardial infarction. *Am. Heart J.* **167**, 637–645.

Bersin, R. M., and Stacpoole, P. W. (1997). Dichloroacetate as metabolic therapy for myocardial ischemia and failure. *Am. Heart J.* **134**, 841–855.

Budanov, A. V., and Karin, M. (2008). p53 target genes sestrin1 and sestrin2 connect genotoxic stress and mTOR signaling. *Cell* **134**, 451–460.

Calvert, J. W., Gundewar, S., Jha, S., Greer, J. J., Bestermann, W. H., Tian, R., and Lefer, D. J. (2008). Acute metformin therapy confers cardioprotection against myocardial infarction via AMPK-eNOS-mediated signaling. *Diabetes* **57**, 696–705.

Ceylan-Isik, A. F., Zhao, P., Zhang, B., Xiao, X., Su, G., and Ren, J. (2010). Cardiac overexpression of metallothionein rescues cardiac contractile dysfunction and endoplasmic reticulum stress but not autophagy in sepsis. *J. Mol. Cell. Cardiol.* **48**, 367–378.

Costa, R., Morrison, A., Wang, J., Manithody, C., Li, J., and Rezaie, A. R. (2012). Activated protein C modulates cardiac metabolism and augments autophagy in the ischemic heart. *J. Thromb. Haemost.* **10**, 1736–1744.

Din, S., Konstandin, M. H., Johnson, B., Emathinger, J., Volkers, M., Toko, H., Collins, B., Ormachea, L., Samse, K., Kubli, D. A., *et al.* (2014). Metabolic dysfunction consistent with premature aging results from deletion of Pim kinases. *Circ. Res.* **115**, 376–387.

Fragasso, G., Piatti, P. M., Monti, L., Palloshi, A., Lu, C., Valsecchi, G., Setola, E., Calori, G., Pozza, G., and Margonato, A. (2002). Acute effects of heparin administration on the ischemic threshold of patients with coronary artery disease: Evaluation of the protective role of the metabolic modulator trimetazidine. *J. Am. Coll. Cardiol.* **39**, 413–419.

Fraser, H., Lopaschuk, G. D., and Clanachan, A. S. (1999). Alteration of glycogen and glucose metabolism in ischaemic and post-ischaemic working rat hearts by adenosine A1 receptor stimulation. *Br. J. Pharmacol.* **128**, 197–205.

Hardie, D. G., and Hawley, S. A. (2001). AMP-activated protein kinase: The energy charge hypothesis revisited. *Bioessays* **23**, 1112–1119.

Hayashi, T., Hirshman, M., Fujii, N., Habinowski, S., Witters, L., and Goodyear, L. (2000). Metabolic stress and altered glucose transport: Activation of AMP-activated protein kinase as a unifying coupling mechanism. *Diabetes* **49**, 527–531.

Johnson, M. T., Mahmood, S., Hyatt, S. L., Yang, H. S., Soloway, P. D., Hanson, R. W., and Patel, M. S. (2001). Inactivation of the murine pyruvate dehydrogenase (Pdha1) gene and its effect on early embryonic development. *Mol. Genet. Metab.* **74**, 293–302.

Kantor, P. F., Lucien, A., Kozak, R., and Lopaschuk, G. D. (2000). The antianginal drug trimetazidine shifts cardiac energy metabolism from fatty acid oxidation to glucose oxidation by inhibiting mitochondrial long-chain 3-ketoacyl coenzyme A thiolase. *Circ. Res.* **86**, 580–588.

Katayama, Y., Fukuchi, T., Mc Kee, A., and Terashi, A. (1998). Effect of hyperglycemia on pyruvate dehydrogenase activity and energy metabolites during ischemia and reperfusion in gerbil brain. *Brain Res.* **788**, 302–304.

Liu, J., Wang, H., Wang, Y., Yin, Y., Wang, L., Liu, Z., Yang, J., Chen, Y., and Wang, C. (2014). Exendin-4 pretreated adipose derived stem cells are resistant to oxidative stress and improve cardiac performance via enhanced adhesion in the infarcted heart. *PLoS One* **9**, e99756

Lopaschuk, G. D. (1999). Optimizing cardiac energy metabolism: A new approach to treating ischaemic heart disease. *Eur. Heart J. Suppl.* **1**, O32–O39.

Louis, A. A., Manousos, I. R., Coletta, A. P., Clark, A. L., and Cleland, J. G. (2002). Clinical trials update: The heart protection study, IONA, CARISA, ENRICHD, ACUTE, ALIVE, MADIT II and REMATCH. *Eur. J. Heart Fail.* **4**, 111–116.

Ma, H., Wang, J., Thomas, D. P., Tong, C., Leng, L., Wang, W., Merk, M., Zierow, S., Bernhagen, J., Ren, J., *et al.* (2010). Impaired macrophage migration inhibitory factor-AMP-activated protein kinase activation and ischemic recovery in the senescent heart. *Circulation* **122**, 282–292.

Ma, Y., and Li, J. (2015). Metabolic shifts during aging and pathology. *Compr. Physiol.* **5**, 667–686.

Ma, Y., Wang, J., Gao, J., Yang, H., Wang, Y., Manithody, C., Li, J., and Rezaie, A. R. (2015). Antithrombin up-regulates AMP-activated protein kinase signalling during myocardial ischaemia/reperfusion injury. *Thromb. Haemost.* **113**, 338–349.

Marsin, A., Rider, M., Deprez, J., and Beauloye, C. (2000). Phosphorylation and activation of heart PFK-2 by AMPK has a role in the stimulation of glycolysis during ischaemia. *Curr. Biol.* **10**, 1247–1255.

Miller, E. J., Li, J., Leng, L., McDonald, C., Atsumi, T., Bucala, R., and Young, L. H. (2008). Macrophage migration inhibitory factor stimulates AMP-activated protein kinase in the ischaemic heart. *Nature* **451**, 578–582.

Miller, E. J., Li, J., Sinusas, K. M., Holman, G. D., and Young, L. H. (2007). Infusion of a biotinylated bis-glucose photolabel: A

new method to quantify cell surface GLUT4 in the intact mouse heart. *Am. J. Physiol. Endocrinol. Metab.* **292**, E1922–E1928.

Morrison, A., Chen, L., Wang, J., Zhang, M., Yang, H., Ma, Y., Budanov, A., Lee, J. H., Karin, M., and Li, J. (2015). Sestrin2 promotes LKB1-mediated AMPK activation in the ischemic heart. *FASEB J.* **29**, 408–417.

Morrison, A., and Li, J. (2011). PPAR-gamma and AMPK–advantageous targets for myocardial ischemia/reperfusion therapy. *Biochem. Pharmacol.* **82**, 195–200.

Morrison, A., Yan, X., Tong, C., and Li, J. (2011). Acute rosiglitazone treatment is cardioprotective against ischemia-reperfusion injury by modulating AMPK, Akt, and JNK signaling in nondiabetic mice. *Am. J. Physiol. Heart Circ. Physiol.* **301**, H895–H902.

Moussa, A., and Li, J. (2012). AMPK in myocardial infarction and diabetes: The yin/yang effect. *Acta Pharm. Sin. B* **2**, 368–378.

Patel, M. S., and Roche, T. E. (1990). Molecular biology and biochemistry of pyruvate dehydrogenase complexes. *FASEB J.* **4**, 3224–3233.

Reed, L. J. (1980). Regulation of mammalian pyruvate dehydrogenase complex by a phosphorylation-dephosphorylation cycle. *Curr. Top. Cell. Regul.* **18**, 95–106.

Russell, R. R., III, Li, J., Coven, D. L., Pypaert, M., Zechner, C., Palmeri, M., Giordano, F. J., Mu, J., Birnbaum, M. J., and Young, L. H. (2004). AMP-activated protein kinase mediates ischemic glucose uptake and prevents postischemic cardiac dysfunction, apoptosis, and injury. *J. Clin. Invest.* **114**, 495–503.

Sakamoto, K., Zarrinpashneh, E., Budas, G. R., Pouleur, A. C., Dutta, A., Prescott, A. R., Vanoverschelde, J. L., Ashworth, A., Jovanovic, A., Alessi, D. R., *et al.* (2006). Deficiency of LKB1 in heart prevents ischemia-mediated activation of AMPKalpha2 but not AMPKalpha1. *Am. J. Physiol. Endocrinol. Metab.* **290**, E780–E788.

Shibata, R., Sato, K., Pimentel, D. R., Takemura, Y., Kihara, S., Ohashi, K., Funahashi, T., Ouchi, N., and Walsh, K. (2005). Adiponectin protects against myocardial ischemia-reperfusion injury through AMPK- and COX-2-dependent mechanisms. *Nat. Med.* **11**, 1096–1103.

Stacpoole, P. W., and Greene, Y. J. (1992). Dichloroacetate. *Diabetes Care* **15**, 785–791.

Taegtmeyer, H., Golfman, L., Sharma, S., Razeghi, P., and van Arsdall, M. (2004). Linking gene expression to function: Metabolic flexibility in the normal and diseased heart. *Ann. N. Y. Acad. Sci.* **1015**, 202–213.

Tian, R., Musi, N., D'Agostino, J., Hirshman, M. F., and Goodyear, L. J. (2001). Increased adenosine monophosphate–activated protein kinase activity in rat hearts with pressure-overload hypertrophy. *Circulation* **104**, 1664–1669.

Tong, C., Morrison, A., Mattison, S., Qian, S., Bryniarski, M., Rankin, B., Wang, J., Thomas, D. P., and Li, J. (2013). Impaired SIRT1 nucleocytoplasmic shuttling in the senescent heart during ischemic stress. *FASEB J.* **27**, 4332–4342.

Ussher, J. R., Koves, T. R., Jaswal, J. S., Zhang, L., Ilkayeva, O., Dyck, J. R., Muoio, D. M., and Lopaschuk, G. D. (2009). Insulin-stimulated cardiac glucose oxidation is increased in high-fat diet-induced obese mice lacking malonyl CoA decarboxylase. *Diabetes* **58**, 1766–1775.

Ussher, J. R., Wang, W., Gandhi, M., Keung, W., Samokhvalov, V., Oka, T., Wagg, C. S., Jaswal, J. S., Harris, R. A., and Clanachan, A. S. (2012). Stimulation of glucose oxidation protects against acute myocardial infarction and reperfusion injury. *Cardiovasc. Res.* **94**, 359–369.

Wang, J., Tong, C., Yan, X., Yeung, E., Gandavadi, S., Hare, A. A., Du, X., Chen, Y., Xiong, H., Ma, C., *et al.* (2013). Limiting cardiac ischemic injury by pharmacological augmentation of macrophage migration inhibitory factor-AMP-activated protein kinase signal transduction. *Circulation* **128**, 225–236.

Wang, J., Yang, L., Rezaie, A. R., and Li, J. (2011). Activated protein C protects against myocardial ischemic/reperfusion injury through AMP-activated protein kinase signaling. *J. Thromb. Haemost.* **9**, 1308–1317.

Winder, W., and Hardie, D. (1999). AMP-activated protein kinase, a metabolic master switch: Possible roles in type 2 diabetes. *Am. J. Physiol. Endocrinol. Metab.* **277**, E1–E10.

Wolff, A. A., Rotmensch, H. H., Stanley, W. C., and Ferrari, R. (2002). Metabolic approaches to the treatment of ischemic heart disease: The clinicians' perspective. *Heart Fail. Rev.* **7**, 187–203.

Yang, K., Zhang, T. P., Tian, C., Jia, L. X., Du, J., and Li, H. H. (2012). Carboxyl terminus of heat shock protein 70-interacting protein inhibits angiotensin II-induced cardiac remodeling. *Am. J. Hypertens.* **25**, 994–1001.

Young, L. H., Renfu, Y., Russell, R., Hu, X., Caplan, M., Ren, J., Shulman, G. I., and Sinusas, A. J. (1997). Low-flow ischemia leads to translocation of canine heart GLUT-4 and GLUT-1 glucose transporters to the sarcolemma in vivo. *Circulation* **95**, 415–422.

Zhang, X. L., Yan, Z. W., Sheng, W. W., Xiao, J., Zhang, Z. X., and Ye, Z. B. (2011a). Activation of hypoxia-inducible factor-1 ameliorates postischemic renal injury via inducible nitric oxide synthase. *Mol. Cell. Biochem.* **358**, 287–295.

Zhang, Y., Zeng, Y., Wang, M., Tian, C., Ma, X., Chen, H., Fang, Q., Jia, L., Du, J., and Li, H. (2011b). Cardiac-specific overexpression of E3 ligase Nrdp1 increases ischemia and reperfusion-induced cardiac injury. *Basic Res. Cardiol.* **106**, 371–383.